Thermochimica Acta, 215 (1993) 47–63
Elsevier Science Publishers B.V., Amsterdam

The thermal decomposition of oxalates. Part 26. A kinetic study of the thermal decomposition of manganese(II) oxalate dihydrate

Xiang Gao and David Dollimore

Department of Chemistry, University of Toledo, Toledo, OH 43606-3390 (USA)

(Received 22 June 1992)

Abstract

The determination of the most probable mechanism function and calculation of the kinetic parameters of decomposition of manganese oxalate have been achieved by a new kinetic analysis procedure under nonisothermal conditions in both dry and wet N_2. The isothermal kinetic analysis has also been performed in each atmosphere. Both the isothermal and nonisothermal analyses showed the most probable mechanism function is first order (F1). The coincidence of results obtained by isothermal and nonisothermal analysis supports the idea that the proposed analysis procedure for nonisothermal conditions is a promising one.

INTRODUCTION

There is a considerable literature devoted to the investigation of the thermal decomposition of manganese(II) oxalate dihydrate. Kinetic studies have been concerned with both dehydration [1, 2] and the subsequent decomposition of the anhydrous oxalate in various atmospheres [3–13] with TG, DSC and DTA. Detailed reaction mechanisms for the latter reaction in inert and oxidizing atmospheres have been proposed [9]. Further, DSC has been used to determine the enthalpy of dehydration of $MnC_2O_4 \cdot 2H_2O$ and the enthalpies of decomposition of the anhydrous oxalate in N_2 and in O_2.

The thermal decompositon of manganese(II) oxalate dihydrate can be considered as occurring in two steps in oxidizing atmosphere or in vacuum, but in three steps in nitrogen followed by admission of air at high temperature. In an oxidizing atmospheres such as air or oxygen, the first step is the endothermic dehydration of manganese(II) oxalate dihydrate, which loses its two water molecules in the temperature range 100–200°C

Correspondence to: D. Dollimore, Department of Chemistry, University of Toledo, Toledo, OH 43606-3390, USA.

[9]; the second step is an exothermic decomposition to MnO_2 in the temperature range 230–330°C [5–7]. In vacuum, the first step is the same as in oxygen, but the temperature range is 100–280°C; the second step is an endothermic decomposition to MnO in the temperature range 300–480°C. In nitrogen, the first and second steps are the same as in vacuum with the same temperature ranges, but at high temperature there is an exothermic oxidation of MnO to MnO_2 with the admission of air [6, 7]. These stages may be represented by the sequence of reactions shown in Table 1.

The surface area has also been measured for the products of different steps using the volumetric adsorption Brunauer–Emmet–Teller (BET) method [3, 6]. The results were used to work out the mechanism and to find out the conditions of temperature treatment for the creation of the maximum surface area. The mechanism of decomposition of manganese(II) oxalate dihydrate was proposed to be as follows: the reaction first undergoes nucleation, followed by growth of particles of product phase, so that it obeys a power law and this is followed by a contracting sphere equation [9]. One point to be noted is that the decomposition of air-dehydrated salt was initiated on all external surface, whereas the vacuum-dehydrated salt showed markedly less change in surface textures when $\alpha < 0.3$ [7]. The activation energies are 70–100 kJ mol^{-1} for dehydration and 86–185 kJ mol^{-1} for decomposition.

TABLE 1

Possible reactions of manganese(II) oxalate [a]

Dehydration	
$MnC_2O_4 \cdot 2H_2O(s) \rightarrow MnC_2O_4(s) + 2H_2O(g)$	(1)
Decomposition	
$MnC_2O_4(s) \rightarrow MnO(s) + CO(g) + CO_2(g)$	(2)
$MnC_2O_4(s) \rightarrow \frac{1}{3}Mn_3O_4(s) + \frac{4}{3}CO(g) + \frac{2}{3}CO_2(g)$	(3)
$MnC_2O_4(s) \rightarrow \frac{1}{2}Mn_2O_3(s) + \frac{3}{2}CO(g) + \frac{1}{2}CO_2(g)$	(4)
Oxidation	
$MnO(s) + \frac{1}{4}O_2(g) \rightarrow \frac{1}{2}Mn_2O_3(s)$	(5)
$MnO(s) + \frac{1}{6}O_2(g) \rightarrow \frac{1}{3}Mn_3O_4(s)$	(6)
$\frac{1}{3}Mn_3O_4(s) + \frac{1}{12}O_2(g) \rightarrow \frac{1}{2}Mn_2O_3(s)$	(7)
$MnC_2O_4(s) + \frac{3}{4}O_2(g) \rightarrow \frac{1}{2}Mn_2O_3(s) + 2CO_2(g)$	(8)
$MnC_2O_4(s) + O_2(g) \rightarrow MnO_2(s) + 2CO_2(g)$	(9)

[a] Ref. 13.

TABLE 2

Experimentally measured data for reactions of manganese(II) oxalate dihydrate: entahalpies (from DSC data) and weight loss [a]

Reaction	ΔH (kJ mol^{-1}) [b]	Loss (mass%)
Dehydration	130 ± 5	19.5 ± 0.2
Decomposition	250 ± 25	58.5 ± 0.5
Oxidation	−300 ± 10	52.0 ± 0.5

[a] Ref. 13. [b] Per mole of dihydrate.

Table 2 shows the enthalpies of the various stages in the dehydration and decomposition of manganese oxalate dihydrate.

This present detailed study allows the determination of the kinetic process of decomposition of $MnC_2O_4 \cdot 2H_2O$ for both identification of mechanism functions and calculation of kinetic parameters.

EXPERIMENTAL

Materials

Manganese oxalate dihydrate was supplied commercially (Johnson Matthey Electronics). The salt is a fine white powder, chemically pure, and was used without further purification.

Techniques

Decomposition experiments were carried out in both dry nitrogen atmosphere and nitrogen atmosphere with water vapor, using the Du Pont 1090 thermogravimetric analyzer, which has a temperature heating rate from 1 to 100°C min^{-1} and an isothermal control between 0 and 1200°C with an accuracy of 0.1°C. All experiments were carried out with a sample size of 16.5 + 0.3 mg.

Isothermal experiment were carried out at 385.5, 399.0, 410.5, 418.0 and 426.0°C in dry N_2 and 370.0, 388.0, 402.5, 409.7 and 417.5°C in wet N_2 for the decomposition. Nonisothermal decompositions were carried out with heating rates of 4.88, 10.0, 17.3, 25.2 and 53.2°C min^{-1}.

METHODOLOGY

Integral and differential methods were used in analyzing the data to identify the reaction kinetic mechanism and calculate the kinetic parameters for both isothermal and nonisothermal conditions.

For isothermal conditions, the rate expression can be written as

$$G(\alpha) = kt \qquad \text{(integral form)} \tag{10}$$

$$(\mathrm{d}\alpha/\mathrm{d}t) = kf(\alpha) \qquad \text{(differential form)} \tag{11}$$

where α is the fraction decomposed.

For a given isothermal run at T_i, the constant $k(T_i)$ can be calculated from the TG curve using either of these two equations. Normally experiments are performed at five or more isothermal temperatures. There is a certain $k(T_i)$ and certain $f(\alpha)$ or $G(\alpha)$ for each T_i. If $f(\alpha)$ or $G(\alpha)$ are all the same for each T_i, then

$$\ln[k(T_i)] = \ln A - E/RT_i \tag{12}$$

and eqn. (12) can be used to obtain the kinetic parameters E and A.

For nonisothermal conditions, a differential rate expression [14] can be written

$$\ln[(\mathrm{d}\alpha/\mathrm{d}t)/f(\alpha)] = \ln A - E/RT \qquad \text{(differential form)} \tag{13}$$

where

$$E = \text{slope} \times R \tag{14}$$

and

$$A = \exp(\text{intercept}) \tag{15}$$

Alternatively, an integral approach might be used to give the equation [15]

$$\ln[G(\alpha)/1.921503T] = \ln(AE/BR) + 3.7720501 - 1.921503 \ln E - E/RT \qquad \text{(integral form)} \tag{16}$$

where

$$E = \text{slope} \times R \tag{17}$$

and

$$A = \exp(\text{intercept} - 3.772051 + 1.9215031 \ln E) \times BR/E \tag{18}$$

where E = activation energy, B = heating rate, A = frequency factor, and $\mathrm{d}\alpha/\mathrm{d}t$ = the rate of conversion, α = fraction of conversion, $G(\alpha)$ and $f(\alpha)$ are the most probable mechanism functions. Table 3 shows the most common forms of $G(\alpha)$ and $f(\alpha)$. We want to identify the most probable mechanism functions among these forms with eqns. (10), (11), (13) and (16), each of which has the form of $Y = aX + b$. We can therefore obtain data from the single TG curve to test the functions $G(\alpha)$ and $f(\alpha)$ listed in Table 3, the one which has the best linearity would be considered as the most probable mechanism function.

TABLE 3

The common forms of $f(\alpha)$ and $G(\alpha)$

Function group	Mechanism		$G(\alpha)$	$f(\alpha)$
Accelerated α–t *curve*	P1	Power law	$\alpha^{1/4}$	$4\alpha^{3/4}$
			$\alpha^{1/3}$	$3\alpha^{2/3}$
			$\alpha^{1/2}$	$2\alpha^{1/2}$
			α	1
			$\alpha^{2/3}$	$\frac{2}{3}\alpha^{-1/2}$
	E1	Exponential law	$\ln \alpha$	α
S-shaped α–t *curve*	A1.5	Avrami–Erofeev	$[-\ln(1-\alpha)]^{2/3}$	$\frac{3}{2}(1-\alpha)[-\ln(1-\alpha)]^{1/3}$
	A2	Avrami–Erofeev	$[-\ln(1-\alpha)]^{1/2}$	$2(1-\alpha)[-\ln(1-\alpha)]^{1/2}$
	A3	Avrami–Erofeev	$[-\ln(1-\alpha)]^{1/3}$	$3(1-\alpha)[-\ln(1-\alpha)]^{2/3}$
	A4	Avrami–Erofeev	$[-\ln(1-\alpha)]^{1/4}$	$4(1-\alpha)[-\ln(1-\alpha)]^{3/4}$
	B1	Prout–Tompkins	$\ln[\alpha/(1-\alpha)]$	$\alpha(1-\alpha)$
			$[-\ln(1-\alpha)]^{2}$	$\frac{1}{2}(1-\alpha)[-\ln(1-\alpha)]^{-1}$
			$[-\ln(1-\alpha)]^{3}$	$\frac{1}{3}(1-\alpha)[-\ln(1-\alpha)]^{-2}$
			$[-\ln(1-\alpha)]^{4}$	$\frac{1}{4}(1-\alpha)[-\ln(1-\alpha)]^{-3}$
Decelerated α–t *curve*	R2	Abstract surface	$1-(1-\alpha)^{1/2}$	$2(1-\alpha)^{1/2}$
	R3	Abstract volume	$1-(1-\alpha)^{1/3}$	$3(1-\alpha)^{2/3}$
	D1	1-D diffusion	α^{2}	$\frac{1}{2}\alpha-1$
	D2	2-D diffusion	$(1-\alpha)\ln(1-\alpha)+\alpha$	$-[\ln(1-\alpha)]^{-1}$
	D3	3-D diffusion	$[1-(1-\alpha)^{1/3}]^{2}$	$\frac{3}{2}[1-(1-\alpha)^{1/3}]^{-1}(1-\alpha)^{2/3}$
	D4	Ginstling–Brouns	$(1-2\alpha/3)-(1-\alpha)^{2/3}$	$\frac{3}{2}[1-(1-\alpha)^{1/3}]^{-1}$
	F1	First order	$-\ln(1-\alpha)$	$1-\alpha$
	F2	Second order	$1/(1-\alpha)$	$(1-\alpha)^{2}$
	F3	Third order	$[1/(1-\alpha)]^{2}$	$\frac{1}{2}(1-\alpha)^{3}$
Extensions			$1-(1-\alpha)^{1/4}$	$4(1-\alpha)^{3/4}$
			$(1-\alpha)^{-1/2}$	$\frac{1}{2}(1-\alpha)^{-2/3}$
			$[(1-\alpha)^{-1/3}-1]^{2}$	$\frac{3}{2}(1-\alpha)^{4/3}[(1-\alpha)^{-1/3}-1]^{-1}$
			$[1-(1-\alpha)^{1/3}]^{1/2}$	$6[1-(1-\alpha)^{1/3}]^{1/2}(1-\alpha)^{2/3}$
			$[1-(1-\alpha)^{1/2}]^{1/2}$	$4\{(1-\alpha)[1-(1-\alpha)]^{1/2}\}^{1/2}$
			$1-(1-\alpha)^{2}$	$\frac{1}{2}(1-\alpha)^{-1}$
			$1-(1-\alpha)^{3}$	$\frac{1}{3}(1-\alpha)^{-2}$
			$1-(1-\alpha)^{4}$	$\frac{1}{4}(1-\alpha)^{-3}$

The correlation coefficient r, standard derivation S_{xy} and standard derivation of slope S_b are used to test linearity. The nearer r approaches unity, and the smaller S_{xy} and S_b are, the better the linearity.

It has been pointed out that the most probable mechanism may be altered at different heating rates [16]. Because the heating rate only affects the heat conduction of the sample, the same most probable mechanism should be obtained at different heating rates. It is logical to think that the kinetic parameter should be almost the same at different heating rates if the mechanism is correct. Based on such an assumption, we use a nonisothermal analysis procedure in this study to identify the most probable mechanism of the thermal decomposition of $MnC_2O_4 \cdot 2H_2O$. The procedure is as follows: first select the several mechanisms which have comparable values of r, S_{xy} and S_b at different heating rates; then the mechanism which has the smallest deviation of E and A can be considered as the most probable mechanism. To make sure, we have also tested the equality of the mean values of E and A at different heating rates obtained by two nonisothermal methods (differential and integral) using the statistical analysis.

RESULTS AND DISCUSSIONS

Figures 1 and 2 show the experimental TG curves obtained at the five temperatures mentioned above, in dry N_2 and wet N_2 respectively. Tables 4 and 5 give the regression results for the isothermal decomposition of manganese oxalate dihydrate in both dry N_2 and wet N_2 respectively. From Tables 4 and 5, A1.5, F1 and D3 are the most probable mechanism functions for each single TG curve in dry N_2; and A1.5, F1 and R3 for

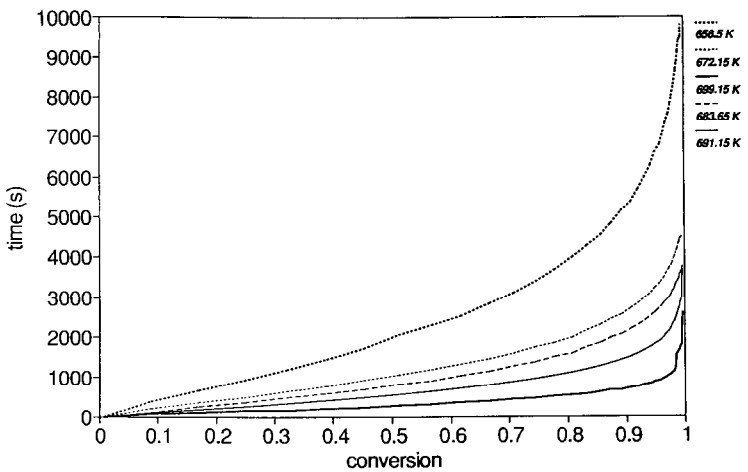

Fig. 1. Experimental TG curves for the isothermal decomposition of $MnC_2O_4 \cdot 2H_2O$ in dry N_2.

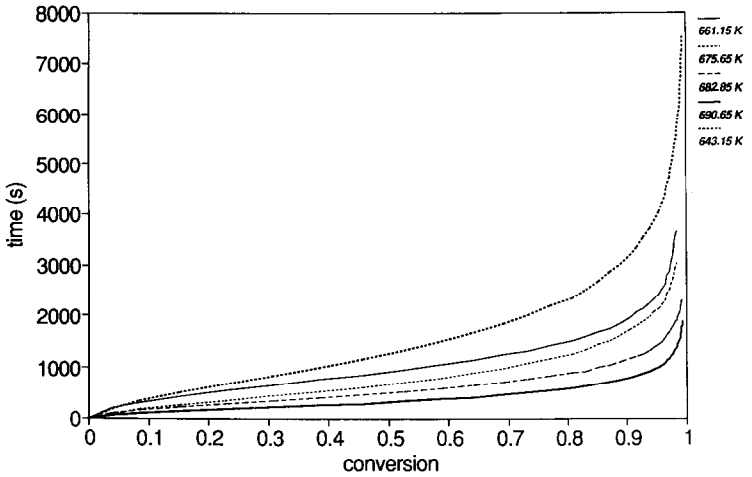

Fig. 2. Experimental TG curves for the isothermal decomposition of $MnC_2O_4 \cdot 2H_2O$ in wet N_2.

each single TG curve in wet N_2. However, the regression factor is the largest, and S_{xy}, S_b are smallest for F1 mechanisms both in dry N_2 and wet N_2 when we calculated E and A using eqn. (12), so F1 is chosen as the most probable mechanism function both in dry and wet N_2.

Figures 3 and 4 give the experimental TG and DTG curves of $MnC_2O_4 \cdot 2H_2O$ decomposed under rising temperature conditions in dry

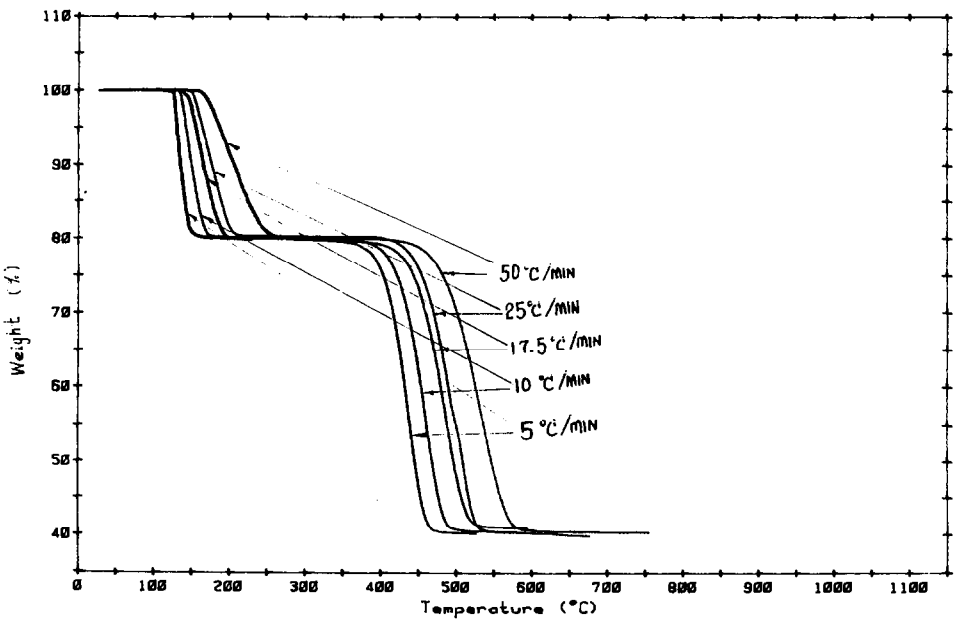

Fig. 3. Experimental TG curves for the nonisothermal decomposition of $MnC_2O_4 \cdot 2H_2O$ in dry N_2.

TABLE 4

The regression results for the isothermal decomposition of $MnC_2O_2 \cdot 2H_2O$ in wet N_2

Most probable mechanism	Isothermal temperature (K)					
	643.15		661.15		675.65	
	r	S	r	S	r	S
A1.5	0.999	0.044	0.999	0.055	0.987	0.137
	0.995	0.032	0.997	0.031	0.993	0.031
F1	0.998	0.186	0.994	0.053	0.997	0.102
	0.995	0.032	0.989	0.031	0.987	0.030
R3	0.996	0.038	0.991	0.051	0.979	0.067
	0.995	0.032	0.995	0.031	0.994	0.030

N_2; Figs. 5 and 6 give the experimental TG and DTG curves of the substances under rising temperature conditions in wet N_2.

Tables 6 and 7 are the regression results for nonisothermal conditions in both dry and wet N_2. From Tables 6 and 7, the most probable mechanism functions are F1 and D3 for both dry and wet N2. Figures 7 and 8 show the degree of linearity which exists between the experimental data and the F1 and D3 functions in dry N_2 when the heating rate is 25.2°C min^{-1}, as do Figs. 9 and 10 for the same experiments in wet N_2. From a single curve one cannot tell which one is better. From Tables 6 and 7, we find that the linearity of F1 is better than that of D3 using the integral method by comparing the three parameters r, S_{xy}, S_b; but D3 is better than F1 using the differential method. The problem is to determine which is the most probable mechanism function. We found that the E and A values are

TABLE 5

The regression results for the isothermal decomposition of $MnC_2O_4 \cdot 2H_2O$ in dry N_2

Most probable mechanism	Isothermal temperature (K)					
	658.5		672.15		683.65	
	r	S	r	S	r	S
A1.5	0.998	0.071	0.999	0.051	0.998	0.061
	0.998	0.015	0.998	0.035	0.994	0.029
F1	0.996	0.136	0.993	0.182	0.991	0.220
	0.994	0.028	0.993	0.036	0.992	0.029
D3	0.993	0.041	0.986	0.045	0.987	0.041
	0.974	0.029	0.974	0.036	0.938	0.024

682.85		690.65		Activation energy (kJ)	Frequency factor	r
r	S	r	S			
0.990	0.141	0.977	0.203	107.5	2.04×10^4	0.917
0.990	0.035	0.978	0.006	145.7	2.56×10^0	0.982
0.998	0.114	0.993	0.203	130.2	1.78×10^7	0.993
0.956	0.035	0.953	0.023	176.4	6.67×10^{10}	0.995
0.974	0.072	0.955	0.091	101.4	2.07×10^4	0.922
0.955	0.035	0.951	0.019	160.0	1.21×10^9	0.989

much closer for F1 at different heating rates than are those for D3. Furthermore, if the mechanism is correct, the E and A values calculated from the differential and integral methods should also be the same. Table 8 gives an estimate of the difference between the two mean values of E and A obtained by the differential and integral methods. From Table 8 it is found that there is a good probability of agreement for the two mean values of E and A being equal with the integral and differential methods for the F1 mechanism, but this is not the case for the D3 mechanism. Comparison of the E and A values obtained by the isothermal and nonisothermal methods, also tells us that the E and A values are much closer for F1 than for D3 (see Table 9). Logicially, it is concluded that F1 is the most probable mechanism for the decomposition of $MnC_2O_4 \cdot 2H_2O$, in both dry and wet N_2.

691.15		699.15		Activation energy (kJ)	Frequency factor	r
r	S	r	S			
0.973	0.127	0.987	0.042	149.1	2.01×10^8	0.970
0.991	0.028	0.989	0.029	165.5	4.56×10^9	0.970
0.987	0.264	0.998	0.013	155.3	1.08×10^9	0.979
0.983	0.028	0.997	0.029	180.3	7.41×10^{10}	0.975
0.981	0.059	0.990	0.052	153.8	1.21×10^8	0.975
0.901	0.028	0.955	0.029	239.6	3.17×10^{14}	0.949

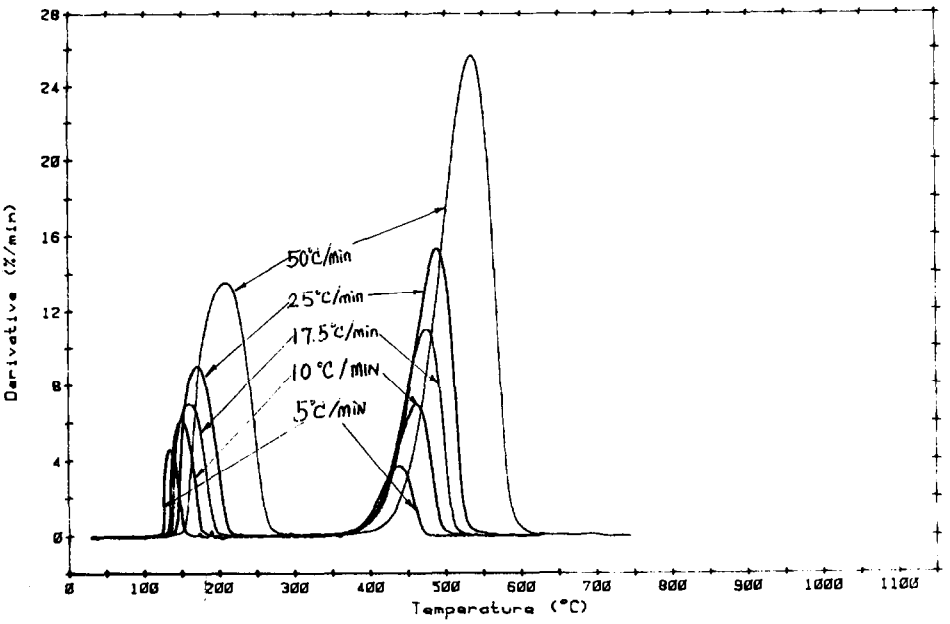

Fig. 4. Experimental DTG curves for the nonisothermal decomposition of $MnC_2O_4 \cdot 2H_2O$ in dry N_2.

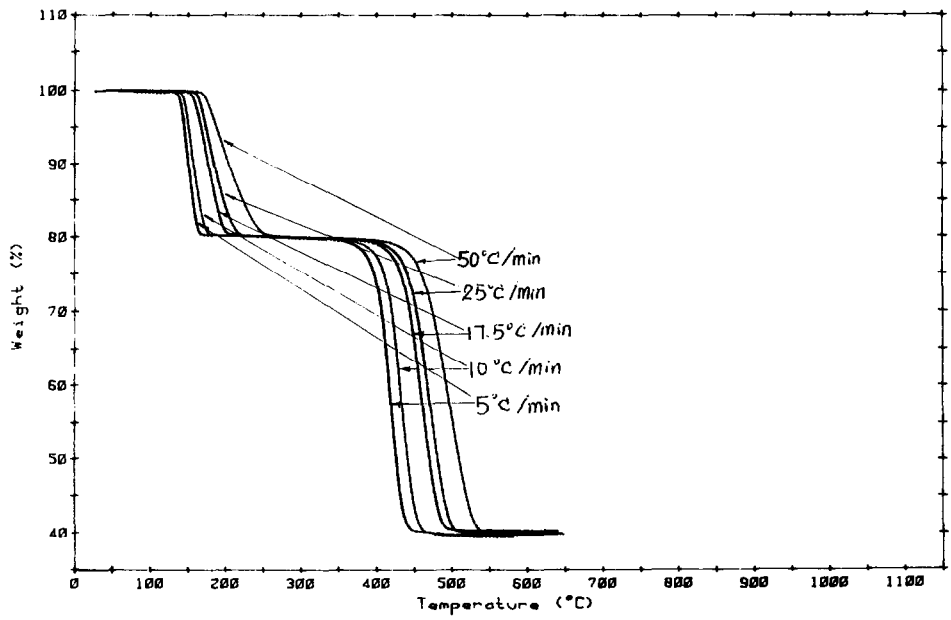

Fig. 5. Experimental TG curves for the nonisothermal decomposition of $MnC_2O_4 \cdot 2H_2O$ in wet N_2.

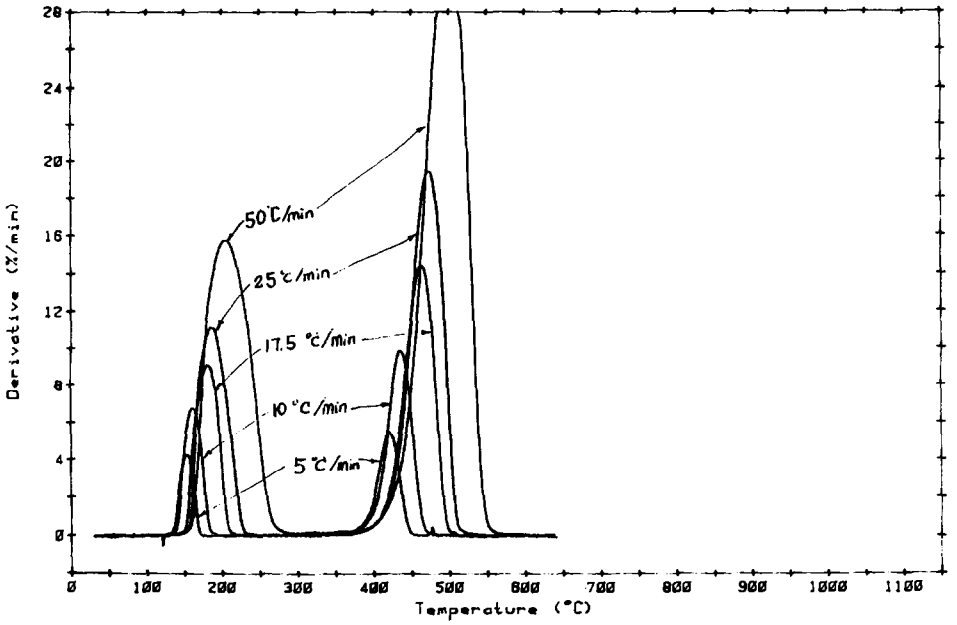

Fig. 6. Experimental DTG curves for the nonisothermal decomposition of $MnC_2O_4 \cdot 2H_2O$ in wet N_2.

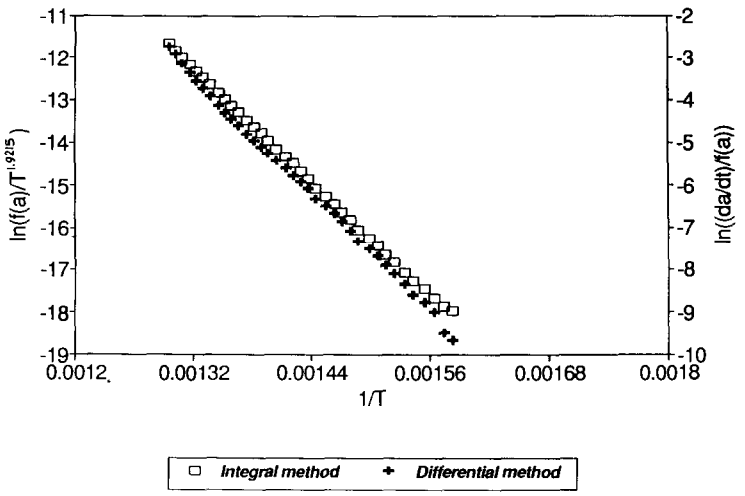

Fig. 7. Regression plot for the decomposition of $MnC_2O_4 \cdot 2H_2O$ in dry N_2; heating rate = 25.2°C min^{-1}, F1.

TABLE 6

The regression results for nonisothermal decomposition of $MnC_2O_4 \cdot 2H_2O$ in dry N_2

Heating rate ($K\,min^{-1}$)	Most probable mechanisms with integral method									
	F1: $f(\alpha) = 1 - \alpha$					D3: $f(\alpha) = 1.5[1 - (1 - \alpha)^{1/3}]^{-1}(1 - \alpha)^{2/3}$				
	E (kJ)	A	r	S_{yx}	S_b	E (kJ)	A	r	S_{yx}	S_b
4.88	155.39	6.10×10^8	0.9814	0.4675	4798.2	290.01	3.60×10^{17}	0.9810	0.8741	8971.5
10.0	174.68	1.58×10^{10}	0.9922	0.3009	3442.2	319.42	2.57×10^{19}	0.9856	0.7271	8318.1
17.3	195.85	5.36×10^{11}	0.9943	0.2672	3511.2	363.84	2.66×10^{22}	0.9864	0.7357	9667.8
25.2	182.18	4.63×10^{10}	0.9967	0.2174	2267.6	339.55	2.51×10^{20}	0.9910	0.6397	6670.5
53.2	173.59	9.59×10^9	0.9987	0.1274	1447.2	327.36	1.54×10^{19}	0.9961	0.3828	4348.3
Average	176.38	1.87×10^{10}	0.9927	0.2760	3093.2	328.36	6.22×10^{19}	0.9880	0.6719	7595.2
Heating rate ($K\,min^{-1}$)	Most probable mechanisms with differential method									
	F1: $f(\alpha) = 1 - \alpha$					D3: $f(\alpha) = 1.5[1 - (1 - \alpha)^{1/3}]^{-1}(1 - \alpha)^{2/3}$				
	E (kJ)	A	r	S_{yx}	S_b	E (kJ)	A	r	S_{yx}	S_b
4.88	150.57	1.70×10^8	0.9570	2.7811	28 572	347.07	1.78×10^{22}	0.9774	3.4756	35 706
10.0	150.40	1.79×10^8	0.9214	2.6817	30 706	387.34	5.92×10^{24}	0.9873	3.5972	41 190
17.3	149.57	1.89×10^8	0.9211	2.4773	32 584	404.50	5.12×10^{25}	0.9863	3.4535	45 425
25.2	159.39	8.31×10^8	0.9509	2.4238	22 529	397.89	8.76×10^{24}	0.9932	3.4752	36 273
53.2	174.26	7.57×10^9	0.9872	1.5756	17 912	397.77	2.73×10^{22}	0.9975	0.3916	4 452
Average	156.84	5.14×10^8	0.9475	2.3881	26 461	387.21	1.05×10^{24}	0.9883	2.8786	32 609

TABLE 7

The regression results for the nonisothermal decomposition of $MnC_2O_4 \cdot 2H_2O$ in wet N_2

Heating rate ($K\,min^{-1}$)	Most probable mechanisms with integral method									
	F1: $f(\alpha) = 1 - \alpha$					D3: $f(\alpha) = 1.5[1-(1-\alpha)^{1/3}]^{-1}(1-\alpha)^{2/3}$				
	E (kJ)	A	r	S_{yx}	S_b	E (kJ)	A	r	S_{yx}	S_b
4.80	232.47	1.06×10^{14}	0.9907	0.3048	4780.2	422.28	1.53×10^{28}	0.9869	0.6461	10 132
9.67	212.29	1.25×10^{13}	0.9864	0.3847	5253.2	379.78	3.69×10^{24}	0.9832	0.7716	10 536
17.4	219.65	4.83×10^{13}	0.9940	0.2262	3702.6	403.34	4.84×10^{25}	0.9930	0.4367	7 147.8
25.2	231.89	2.91×10^{14}	0.9954	0.2111	3507.7	423.52	6.43×10^{26}	0.9914	1.1878	18 730
50.0	215.47	1.34×10^{13}	0.9992	0.0940	1533.2	394.58	1.46×10^{24}	0.9953	0.3595	5 867.3
Average	222.41	4.78×10^{13}	0.9931	0.2442	3755.4	404.70	7.61×10^{25}	0.9900	0.6803	10 482
Heating rate ($K\,min^{-1}$)	Most probable mechanisms with differential method									
	F1: $f(\alpha) = 1 - \alpha$					D3: $f(\alpha) = 1.5[1-(1-\alpha)^{1/3}]^{-2}(1-\alpha)^{2/3}$				
	E (kJ)	A	r	S_{yx}	S_b	E (kJ)	A	r	S_{yx}	S_b
4.80	203.51	4.29×10^{12}	0.9093	2.7195	42 691	511.51	2.15×10^{35}	0.9828	3.2959	51 744
9.67	190.01	3.79×10^{11}	0.9043	3.0317	41 499	465.93	2.33×10^{31}	0.9792	3.6240	49 531
17.4	212.61	9.25×10^{12}	0.9559	1.4834	24 299	510.51	6.39×10^{33}	0.9913	0.6473	10 630
25.2	214.29	1.35×10^{13}	0.9546	1.4318	23 808	520.42	1.29×10^{34}	0.9920	2.7567	45 836
50.0	216.01	1.36×10^{13}	0.9872	1.5756	17 912	488.58	1.32×10^{31}	0.9959	0.4073	6 654
Average	207.20	4.87×10^{12}	0.9422	2.0484	30 041	499.39	1.40×10^{33}	0.9882	2.1462	32 879

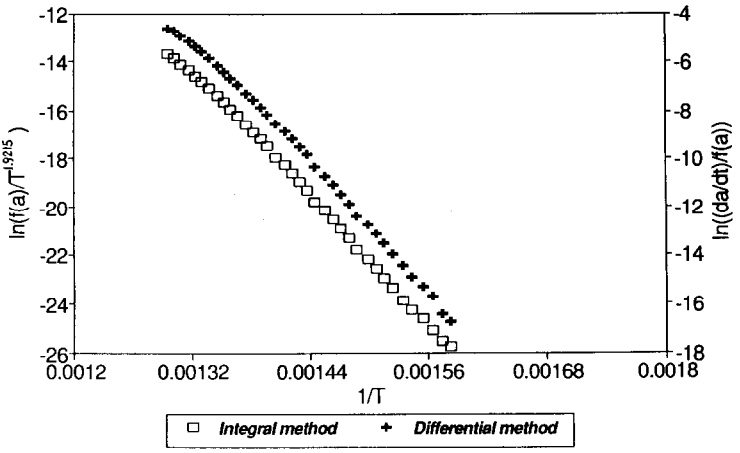

Fig. 8. Regression plot for the decomposition of $MnC_2O_4 \cdot 2H_2O$ in dry N_2; heating rate = 25.2° min^{-1}, D3.

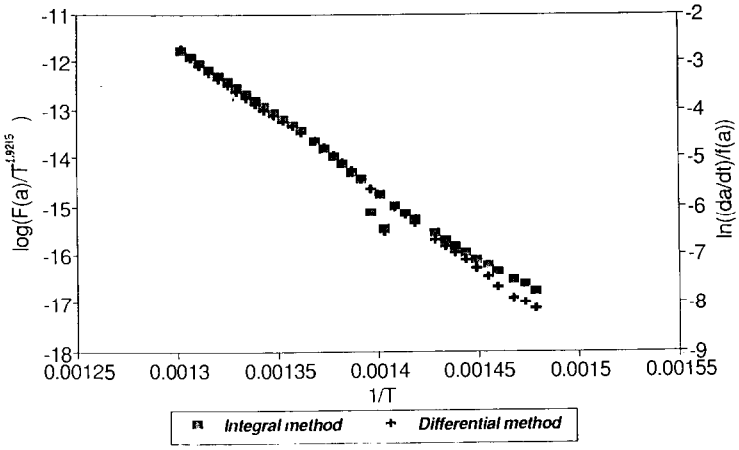

Fig. 9. Regression plot for the decomposition of $MnC_2O_4 \cdot 2H_2O$ in wet N_2; heating rate = 25.2°C min^{-1}, F1.

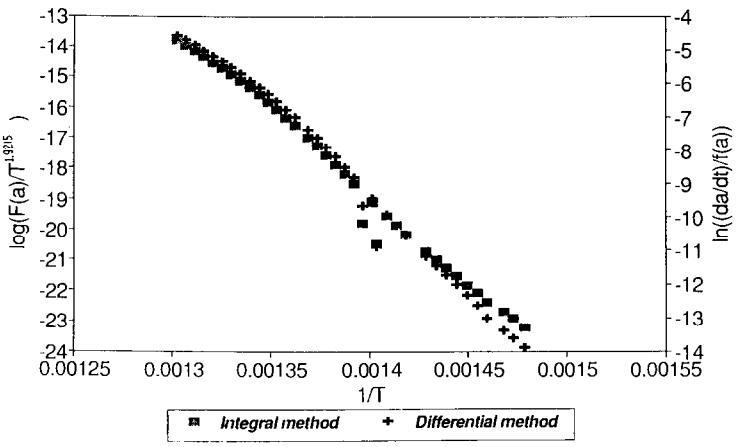

Fig. 10. Regression plot for the decomposition of $MnC_2O_4 \cdot 2H_2O$ in wet N_2; heating rate = 25.2°C min^{-1}, D3.

TABLE 8

Estimated difference between two mean values (confidence interval 95%)

Mechanism	Integral method	Differential method	Difference between two mean values
Dry N_2			
F1	$E_1 = 176.38$ kJ	$E_2 = 156.84$ kJ	$-0.2947 < E_1 - E_2 < 39.32$
	$s_1 = 14.69$	$s_2 = 10.53$	
	$\ln A_1 = 23.65$	$\ln A_2 = 20.25$	$-0.3464 < \ln A_1 - \ln A_2 < 6.4535$
	$s_1 = 2.4633$	$s_2 = 1.643$	
D3	$E_1 = 328.04$ kJ	$E_2 = 387.21$ kJ	$22.45 < E_2 - E_1 < 95.89$
	$s_1 = 27.09$	$s_2 = 23.1$	
	$\ln A_1 = 45.58$	$\ln A_2 = 55.61$	$4.6189 < \ln A_2 - \ln A_1 < 15.44$
	$s_1 = 4.12$	$s_2 = 3.249$	
Wet N_2			
F1	$E_1 = 222.41$ kJ	$E_2 = 207.20$ kJ	$-0.5321 < E_1 - E_2 < 29.01$
	$s_1 = 9.344$	$s_2 = 10.79$	
	$\ln A_1 = 31.03$	$\ln A_2 = 29.21$	$-0.0163 < \ln A_1 - \ln A_2 < 3.601$
	$s_1 = 0.8995$	$s_2 = 1.5$	
D3	$E_1 = 404.7$ kJ	$E_2 = 499.39$ kJ	$60.95 < E_2 - E_1 < 128.42$
	$s_1 = 18.36$	$s_2 = 27.075$	
	$\ln A_1 = 59.59$	$\ln A_2 = 76.32$	$10.88 < \ln A_2 - \ln A_1 < 22.58$
	$s_1 = 3.797$	$s_2 = 4.216$	

TABLE 9

Comparison of E and A values obtained from different methods

Isothermal methods		Nonisothermal methods	
E (kJ)	A	E (kJ)	A
F1 (dry N_2)		*F1 (dry N_2)*	
155.3	1.08×10^9	176.38	1.87×10^{10}
180.3	7.41×10^{10}	156.84	5.14×10^8
F1 (wet N_2)		*F1 (wet N_2)*	
130.2	1.78×10^7	222.41	4.78×10^{13}
176.4	6.67×20^{10}	207.20	4.87×10^{12}
D3 (dry N_2)		*D3 (dry N_2)*	
153.8	1.21×10^8	328.36	6.22×10^{19}
239.6	3.17×10^{14}	387.21	1.05×10^{24}

CONCLUSIONS

(1) The most probable kinetic mechanism function is F1 in both wet and dry N_2 in the heating rate range 5.0–50.0°C min^{-1}. The activation energy $E = 156.84$–176.39 kJ and the frequency factor $A = 5.14 \times 10^8$ to 1.87×10^{10} in dry N_2; $E = 207.20$–222.41 kJ and $A = 4.87 \times 10^{12}$ to 4.78×10^{13} in wet N_2.

(2) Using both integral and differential methods at different heating rates to calculate the kinetic parameters and for determination of the kinetic mechanism function is much better than using only one heating rate. This approach can identify a mechanism which is not really the most probable mechanism but may appear to be so based on a single heating rate.

(3) The study of the isothermal decomposition and the nonisothermal decomposition of manganese oxalate dihydrate shows the same most probable mechanism and closer value of E and A, which supports the use of the proposed method as a promising one.

ACKNOWLEDGMENT

The authors appreciate discussions with Yoke Foo Lee and his help during this study.

REFERENCES

1 B. Topley and M.L. Smith, J. Chem. Soc., (1935) 321.
2 T.B. Flanagan and C.H. Kim, J. Phys. Chem., 66 (1962) 926.
3 D. Dollimore and D. Nicholson, J. Chem. Soc., (1962) 960–965.
4 D. Dollimore, D.L. Griffiths and D. Nicholson, J. Chem. Soc., (1963) 2617–2623.
5 D. Dollimore and K.H. Tonge, in G.M. Schwab (Ed.), Proc. 5th Int. Symp. on the Reactivity of Solids, Elsevier, Amsterdam, 1965, pp. 497–508.
6 D. Dollimore, J. Dollimore and J. Little, J. Chem. Soc. A, (1969) 2946.
7 D. Dollimore and D.L. Griffiths, J. Therm. Anal., (1970) 229–250.
8 D. Dollimore and K.H. Tonge, J. Therm. Anal., 2 (1971) 91–103.
9 M.E. Brown, D. Dollimore and A.K. Galwey, J. Chem. Soc. Faraday Trans. 1, 70 (1974) 1316–1324.
10 M.E. Brown, D. Dollimore and A.K. Galwey, Thermochim. Acta, 21 (1977) 103–110.
11 E.D. Macklen, J. Inorg. Nucl. Chem., 30 (1968) 2689.
12 J.G. Brown, D. Dollimore, J. Dollimore and A.D. Heyes, in T. Gast and R. Robens (Eds.), Progress in Vacuum Microbalance Techniques, Vol. 1, Heyden, London, 1972, pp. 217–235.
13 D. Dollimore, N.M. Guindy, Thermochim. Acta, 58 (1982) 191–198.
14 D. Dollimore, G.R. Heal and B.W. Krupay, Thermochim. Acta, 24 (1978) 293–306.
15 P.M. Madhusudanan, K. Krishnan and K.N. Ninan, Thermochim. Acta, 97 (1986) 189.
16 X. Gao and D. Dollimore, in preparation.

APPENDIX

(1) For testing linearity, the regression equation is used in the form

$$Y = a + bX \tag{A1}$$

where

$$b = \left[\sum X_i Y_i - \left(\sum X_i\right)\left(\sum Y_i\right)/n\right] / \left[\sum X_i^2 - \left(\sum X_i\right)^2/n\right] \tag{A2}$$

and

$$a = Y - bX \tag{A3}$$

and

$$Y = \sum Y_i/n \tag{A4}$$

$$X = \sum X_i/n \tag{A5}$$

The statistical parameters used here are r, S_{xy}, S_b; their definitions have been mentioned previously. Their mathematical expressions are

$$r = \left[\sum (X_i - X)(Y_i - Y)\right] / \left[\sum (X_i - X)^2 \sum (Y_i - Y)^2\right]^{1/2} \tag{A6}$$

$$S_{xy} = \left\{\sum [Y_i - (bX_i + a)]^2/(n-2)\right\}^{1/2} \tag{A7}$$

$$S_b = S_{xy} / \left[\sum (X_i - X)^2\right]^{1/2} \tag{A8}$$

where X_i and Y_i are the ith experimental data and n is the number of experimental data.

(2) The statistic estimation of the difference between the mean activated energy, mean frequency factor of different kinetic methods with the same mechanism.

Confidence Interval for $\mu_1 - \mu_2$; $\sigma_1^2 = \sigma_2^2$ but unknown:
if $\bar{x}_1$ and $\bar{x}_2$ are the means of independent random samples of size n_1 and n_2, respectively, from approximate normal populations with unknown but equal variances, a $(1-\alpha)100\%$ confidence interval for $\mu_1 - \mu_2$ is given by

$$(\bar{x}_1 - \bar{x}_2) - t_{\alpha/2} s_p \sqrt{\frac{1}{n_1} + \frac{1}{n_2}} < \mu_1 - \mu_2 < (\bar{x}_1 - \bar{x}_2) + t_{\alpha/2} s_p \sqrt{\frac{1}{n_1} + \frac{1}{n_2}}$$

where s_p is the pooled estimate of the population standard deviation and $t_{\alpha/2}$ is the t-value with $v = n_1 + n_2 - 2$ degrees of freedom, leaving an area of $\alpha/2$ to the right.